THE ASTROPHYSICAL JOURNAL, 241:425–441, 1980 October 1

DISK-SATELLITE INTERACTIONS

PETER GOLDREICH
California Institute of Technology
AND
SCOTT TREMAINE
Institute for Advanced Study, Princeton, New Jersey
Received 1980 January 7; accepted 1980 April 9

ABSTRACT

We calculate the rate at which angular momentum and energy are transferred between a disk and a satellite which orbit the same central mass. A satellite which moves on a circular orbit exerts a torque on the disk only in the immediate vicinity of its Lindblad resonances. The direction of angular momentum transport is outward, from disk material inside the satellite's orbit to the satellite and from the satellite to disk material outside its orbit. A satellite with an eccentric orbit exerts a torque on the disk at corotation resonances as well as at Lindblad resonances. The angular momentum and energy transfer at Lindblad resonances tends to increase the satellite's orbit eccentricity whereas the transfer at corotation resonances tends to decrease it. In a Keplerian disk, to lowest order in eccentricity and in the absence of nonlinear effects, the corotation resonances dominate by a slight margin and the eccentricity damps. However, if the strongest corotation resonances saturate due to particle trapping, then the eccentricity grows.

We present an illustrative application of our results to the interaction between Jupiter and the protoplanetary disk. The angular momentum transfer is shown to be so rapid that substantial changes in both the structure of the disk and the orbit of Jupiter must have taken place on a time scale of a few thousand years.

Subject headings: hydrodynamics — planets: Jupiter — planets: satellites — solar system: general

I. INTRODUCTION

The main purpose of this paper is to evaluate the transfer of angular momentum and energy between a disk and a satellite in order to determine their mutual evolution. Our results are applicable to a variety of systems: the rings of Saturn (Goldreich and Tremaine 1978*b*, henceforth GT1), the rings of Uranus (Goldreich and Tremaine 1979*a*), accretion disks in close binary systems (Lin and Papaloizou 1979), and the protoplanetary nebula (cf. § VI).

The plan of the paper is as follows. In § II we calculate the angular momentum and energy transfer due to the torques which the satellite exerts on the disk at Lindblad and corotation resonances. The orbital evolution of a satellite and a neighboring narrow ring is explicitly evaluated. Section III contains an alternate derivation of the results obtained in § II, based on a single close encounter between the satellite and each ring particle. The cutoff in the torque at Lindblad resonances which occurs close to the satellite is accurately computed in § IV. Next, in § V we describe additional features of disk-satellite interactions which are relevant in applications to planetary rings. Section VI includes an illustrative application to the mutual evolution of Jupiter's orbit and the protoplanetary gas disk. Finally, § VII contains a summary and guide to the most important equations.

From time to time we will refer to Goldreich and Tremaine (1978*c*) as GT2, and to Goldreich and Tremaine (1979*b*) as GT3.

II. STEADY-STATE INTERACTIONS AT RESONANCES

a) The Disk

For our purposes, it suffices to consider a two-dimensional disk which lies in the equatorial plane of a cylindrical coordinate system (r, θ, z). The unperturbed disk is azimuthally symmetric and rotates with angular velocity $\Omega(r) > 0$. Oort's parameters $A(r)$, $B(r)$ and the epicyclic frequency $\kappa(r)$ are defined by

$$A(r) \equiv \frac{r}{2}\frac{d\Omega}{dr}, \qquad B(r) \equiv \Omega(r) + A(r), \qquad \kappa^2(r) \equiv \frac{1}{r^3}\frac{d}{dr}[r^2\Omega(r)]^2 = 4B(r)\Omega(r). \tag{1}$$

The validity of most of our results does not depend upon the nature and composition of the disk material. It may be a fluid, a collisionless gas, or a collection of macroscopic particles. However, the magnitude of the typical random particle velocity, denoted by c, is assumed to be much smaller than the circular velocity, $c \ll \Omega r$, as is observed in planetary rings. Also, the surface mass density Σ is constrained by $G\Sigma \ll \Omega^2 r$, which implies that the disk makes a negligible contribution to the unperturbed gravity field. Thus, we consider only disks which orbit some central rigid body, whose mass we denote by M_p. Some other restrictions on the validity of our results are discussed in § V.

The most important special case is the nearly Keplerian disk for which $\Omega^2(r) \approx GM_p/r^3$, $A/\Omega \approx -\frac{3}{4}$, $B/\Omega \approx \frac{1}{4}$, and $\kappa/\Omega \approx 1$.

b) *The Satellite*

The satellite orbit is characterized by the elements a and e and is assumed to lie in the disk plane. We define a such that the instantaneous angular velocity is equal to $\Omega(a)$ when the satellite crosses $r = a$. Note that for the Kepler problem a differs from the semimajor axis in order e^2. The eccentricity $e \equiv (r_{\max} - r_{\min})/2a$. For $e \ll 1$, the satellite makes an epicyclic oscillation at angular frequency $\kappa_s \equiv \kappa(a)$ about a guiding center which revolves at the rate $\Omega_s \equiv \Omega(a)$. To first order in e, we may write

$$r_s = a(1 - e\cos\kappa_s t)\,, \qquad \theta_s = \Omega_s t + \frac{2\Omega_s e}{\kappa_s}\sin\kappa_s t \tag{2}$$

(Chandrasekhar 1960). The apse precession rate is given by

$$\frac{d\tilde{\omega}}{dt} = \Omega_s - \kappa_s\,. \tag{3}$$

The perturbation potential due to a satellite of mass M_s reads

$$\phi^s(r, \theta, t) = -\frac{GM_s}{|\boldsymbol{r} - \boldsymbol{r}_s|} + \frac{M_s}{M_p}\Omega^2(r)\boldsymbol{r}_s\cdot\boldsymbol{r}\,. \tag{4}$$

The second term is the indirect part of the potential which arises because the coordinate origin is attached to the central mass.

It is convenient to expand ϕ^s in a Fourier series:

$$\phi^s(r, \theta, t) = \sum_{l=-\infty}^{\infty}\sum_{m=0}^{\infty}\phi^s_{l,m}(r)\cos\{m\theta - [m\Omega_s + (l-m)\kappa_s]t\}\,. \tag{5}$$

For $e \ll 1$, the largest term in $\phi^s_{l,m}$ is proportional to $e^{|l-m|}$. The pattern speed of the l, m potential component is

$$\Omega_{l,m} = \Omega_s + \frac{(l-m)}{m}\kappa_s\,. \tag{6}$$

It is straightforward to calculate $\phi^s_{l,m}$ from equations (2) and (4). To first order in e, the only nonvanishing components are

$$\phi^s_{m,m} = -\frac{GM_s}{2a}(2 - \delta_{m,0})(b^m_{1/2} - f\beta\delta_{m,1})\,, \tag{7}$$

$$\phi^s_{m+1,m} = -\frac{GM_s}{2a}e(2 - \delta_{m,0})\left[\left(\frac{1}{2} + \frac{m\Omega_s}{\kappa_s} + \frac{\beta}{2}\frac{d}{d\beta}\right)b^m_{1/2} - f\beta\left(\frac{3}{2} - \frac{2B_s}{\Omega_s} + \frac{\Omega_s}{\kappa_s}\right)\delta_{m,1}\right], \tag{8}$$

$$\phi^s_{m-1,m} = -\frac{GM_s}{2a}e(2 - \delta_{m,0})\left[\left(\frac{1}{2} - \frac{m\Omega_s}{\kappa_s} + \frac{\beta}{2}\frac{d}{d\beta}\right)b^m_{1/2} - f\beta\left(\frac{3}{2} - \frac{2B_s}{\Omega_s} - \frac{\Omega_s}{\kappa_s}\right)\delta_{m,1}\right]. \tag{9}$$

Here $f \equiv \Omega_s^2 a^3/GM_p$, $\beta \equiv r/a$, $\delta_{m,n}$ is the Kronecker delta function, and $b^m_{1/2}(\beta)$ is the Laplace coefficient,

$$b^m_{1/2}(\beta) \equiv \frac{2}{\pi}\int_0^\pi \frac{\cos m\phi\, d\phi}{(1 - 2\beta\cos\phi + \beta^2)^{1/2}}\,. \tag{10}$$

The terms in $\phi^s_{l,m}$ proportional to $\delta_{m,1}$ arise from the indirect part of the perturbation potential. Equations (7)–(10) are valid for all β.

c) *Torques at Resonances*

Torques are exerted on the disk by $\phi^s_{l,m}$ only in the immediate vicinity of Lindblad and corotation resonances. The former occur where

$$\Omega(r) + \epsilon \frac{\kappa(r)}{m} = \Omega_{l,m}\,, \qquad \epsilon = \pm 1\,, \quad m > 0\,; \tag{11}$$

and the latter where

$$\Omega(r) = \Omega_{l,m}\,, \qquad m > 0\,. \tag{12}$$

We ignore $m = 0$ perturbations since they are axisymmetric and exert no torque. At the Lindblad resonance the epicyclic motion of a particle in a circular orbit is strongly excited, since the perturbation frequency felt by the particle is equal to its epicyclic frequency. At the corotation resonance the angular momentum of a particle in a circular orbit undergoes large changes, since the particle feels a slowly varying azimuthal force. However, the particle's epicyclic motion is not excited. A Keplerian disk of infinite extent has one inner ($\epsilon = -1$) and one outer ($\epsilon = +1$) Lindblad resonance and a single corotation resonance for each $\Omega_{l,m} > 0$ and $m > 1$.

Analytic expressions for the torque are derived in GT3. At a Lindblad resonance $r = r_L$,

$$T^L_{l,m} = -m\pi^2 \left[\Sigma \left(\frac{rdD}{dr} \right)^{-1} \left(\frac{rd\phi^s_{l,m}}{dr} + \frac{2\Omega}{\Omega - \Omega_{l,m}} \phi^s_{l,m} \right)^2 \right]_{r_L}\,, \tag{13}$$

where $D = \kappa^2 - m^2(\Omega - \Omega_{l,m})^2$. Note that the sign of $T^L_{l,m}$ is opposite to that of dD/dr. Thus, angular momentum is removed from the disk at an inner Lindblad resonance and added to it at an outer Lindblad resonance (Lynden-Bell and Kalnajs 1972). At a corotation resonance $r = r_C$,

$$T^C_{l,m} = \frac{m\pi^2}{2} \left[\left(\frac{d\Omega}{dr} \right)^{-1} \frac{d}{dr} \left(\frac{\Sigma}{B} \right) (\phi^s_{l,m})^2 \right]_{r_C}\,. \tag{14}$$

Note that the sign of $T^C_{l,m}$ is that of the gradient of vorticity per unit surface density if $d\Omega/dr < 0$. The torque formulae are valid in the limit that $c \ll \Omega r$, $G\Sigma \ll \Omega^2 r$, and $m \ll \Omega r/c$. The implications of the violation of the last inequality are examined in § IV.

Given a disk and a satellite, the apparatus we have assembled enables us to locate the resonances and to calculate the torques exerted on the disk. This procedure was applied to Saturn's rings in GT1 to provide an explanation for the formation of the Cassini division. Here our goal is slightly different. We are primarily concerned with those resonances which are close to the satellite, i.e., those for which $|r_L - a| \ll a$ and $|r_C - a| \ll a$ or, what is equivalent, $m \gg 1$. In this limit the positions of the resonances are located as shown in Figure 1. Two features are worth commenting on. First, some of the resonances are at $r = a$. Clearly, the linear perturbation theory used to calculate

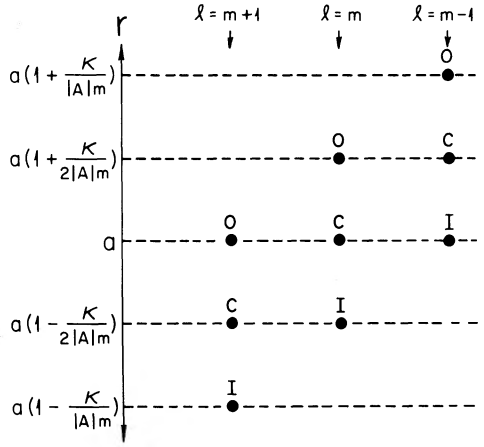

FIG. 1.—The positions of the most important resonances for fixed $m \gg 1$. We only show resonances with $|l - m| \leq 1$ since the perturbing potential from the satellite (cf. eq. [5]) is $\propto e^{|l-m|}$, The symbols O, C, and I denote outer Lindblad resonances, corotation resonances, and inner Lindblad resonances, respectively.

the torques given by equations (13) and (14) is an inadequate tool for these resonances. Second, there is an infinite sequence of resonances of each type $l = m$, $l = m \pm 1$, and each sequence has an accumulation point at $r = a$. The high density of resonances near a leads us to introduce the average torque per radial interval, or torque density, which we denote by $dT^{L}_{l,m}/dr$ or $dT^{C}_{l,m}/dr$.

To compute the torque densities we use equations (7)–(10), (13), and (14) and Figure 1. To evaluate $b^{m}_{1/2}(\beta)$ for $|1 - \beta| \ll 1$ and $m \gg 1$, we note that most of the contribution to the integral in equation (10) comes from $\theta \ll 1$. Thus, we replace $\cos\theta$ by $1 - \theta^2/2$, extend the upper limit to infinity, and set $\beta = 1$ except where it appears in the combination $1 - \beta$. This procedure yields

$$b^{m}_{1/2}(\beta) \approx \frac{2}{\pi} K_0(m|1 - \beta|)\,, \tag{15}$$

where K_ν denotes the modified Bessel function of order ν. Similarly,

$$\frac{db^{m}_{1/2}(\beta)}{d\beta} \approx \operatorname{sgn}(1 - \beta)\frac{2m}{\pi} K_1(m|1 - \beta|)\,, \tag{16}$$

and

$$\frac{d^2 b^{m}_{1/2}(\beta)}{d\beta^2} \approx \frac{2m^2}{\pi}\left[K_0(m|1 - \beta|) + \frac{1}{m|1 - \beta|} K_1(m|1 - \beta|)\right]. \tag{17}$$

The resulting torque densities are

$$\frac{dT^{L}_{m,m}}{dr} = \operatorname{sgn}(r - a)\frac{\kappa^2 r\Sigma}{2^3 A^4}\frac{(GM_s)^2}{(a - r)^4}\{(2\Omega/\kappa)K_0(\kappa/2|A|) + K_1(\kappa/2|A|)\}^2\,, \tag{18}$$

$$\frac{dT^{L}_{m\pm 1,m}}{dr} = \operatorname{sgn}(r - a)\frac{e^2\kappa^4 r^3\Sigma}{2^2 A^6}\frac{(GM_s)^2}{(a - r)^6}\{[1 + (2\Omega/\kappa)^2]K_0(\kappa/|A|) + [|A|/\kappa + 4\Omega/\kappa]K_1(\kappa/|A|)\}^2\,, \tag{19}$$

$$\frac{dT^{C}_{m\pm 1,m}}{dr} = -\frac{e^2\kappa^4 r^3}{2^6|A|^5}\frac{(GM_s)^2}{|a - r|^5}\frac{d}{dr}\left(\frac{\Sigma}{B}\right)\{(2\Omega/\kappa)K_0(\kappa/2|A|) + K_1(\kappa/2|A|)\}^2\,. \tag{20}$$

e) Orbital Variations

Next we investigate the rates of change of a and e due to the interaction between a satellite and a circular ring of radial width Δr and mass M_r. The mean radius and radial width of the ring are subject to the constraints

$$\frac{c}{\Omega r} \ll \frac{|a - r|}{a} \ll 1\,, \qquad \frac{|a - r|^2}{a^2} \ll \frac{\Delta r}{a} \ll \frac{|a - r|}{a}\,. \tag{21}$$

The lower limit on the mean separation between the ring and the satellite orbit is equivalent to the requirement that $m \ll \Omega r/c$ for those $l = m$ and $l = m \pm 1$ resonances which lie within the ring. Our torque equations (13) and (14) are only valid in this limit. The lower limit on the ring width ensures that many resonances of each type fall within the ring boundaries so that the torque density is a meaningful concept. The effects of a wide ring on the satellite orbit may be determined by summing the effects of many narrow rings.

A simple derivation of the perturbation equations for a and e starts with the integrals of the unperturbed satellite orbit. These are the angular momentum

$$H = M_s a^2\Omega \tag{22}$$

and the energy

$$E = \tfrac{1}{2}M_s[(a\Omega)^2 + (ea\kappa)^2] + M_s\Phi(a)\,, \tag{23}$$

where Φ is the unperturbed gravitational potential. The forms of the integrals follow immediately from the definitions of a and e adopted in § II*b*. The expression for H is exact whereas that for E is valid to order e^2. For each ring torque component T_r with pattern speed Ω_p there is a reaction torque on the satellite which changes H and E according to

$$\frac{dH}{dt} = -T_r\,, \tag{24}$$

$$\frac{dE}{dt} = -\Omega_p T_r\,. \tag{25}$$

From equations (22)–(25) and the identities $a\Omega^2 = d\Phi/dr$ and $\kappa^2 - 3\Omega^2 = d^2\Phi/dr^2$, we find

$$\frac{da}{dt} = -\frac{2\Omega T_r}{a\kappa^2 M_s}, \tag{26}$$

$$\frac{de}{dt} = -\left[(\Omega_p - \Omega) - 2e^2\Omega\left(1 + \frac{d\ln\kappa}{d\ln r}\right)\right]\frac{T_r}{M_s e(a\kappa)^2}. \tag{27}$$

Here Ω, κ, and $d\ln\kappa/d\ln r$ are to be evaluated at $r = a$.

The leading contribution to da/dt is due to $dT^{\rm L}_{m,m}/dr$ (eq. [18]). We find

$$\frac{da}{dt} = \mathrm{sgn}\,(a - r)\frac{\Omega G^2 M_s M_r}{8\pi A^4 a(a - r)^4}\left[(2\Omega/\kappa)K_0(\kappa/2|A|) + K_1(\kappa/2|A|)\right]^2, \tag{28}$$

where $M_r \equiv 2\pi\Sigma r\Delta r$.

The computation of de/dt is slightly more subtle. The effect of $dT^{\rm L}_{m,m}/dr$ is smaller than that of $dT^{\rm L}_{m\pm1,m}/dr$ by $\sim|a - r|/a \ll 1$. To ascertain the contribution of $dT^{\rm C}_{m\pm1,m}/$dr, we integrate over the ring holding constant everything but Σ and $|a - r|^{-5}$, the most rapidly varying factors. We find that $dT^{\rm L}_{m\pm1,m}/dr$ and $dT^{\rm C}_{m\pm1,m}/dr$ make comparable contributions to de/dt. The end result is

$$\frac{1}{e}\frac{de}{dt} = \frac{\kappa^2 G^2 M_s M_r}{8\pi|A|^5 a|a - r|^5}\left\{\langle[1 + (2\Omega/\kappa)^2]K_0(\kappa/|A|) + [|A|/\kappa + 4\Omega/\kappa]K_1(\kappa/|A|)\rangle^2 - \frac{|A|}{2B}\langle(2\Omega/\kappa)K_0(\kappa/2|A|) + K_1(\kappa/2|A|)\rangle^2\right\}. \tag{29}$$

The positive first term and the negative second term come from the Lindblad and corotation resonances, respectively.

A numerical evaluation of $a^{-1}da/dt$ and $e^{-1}de/dt$ for the Keplerian disk yields

$$\frac{1}{a}\frac{da}{dt} = 0.798\frac{M_s M_r}{M_p^2}\left(\frac{a}{a - r}\right)^4\Omega\,\mathrm{sgn}\,(a - r), \tag{30}$$

$$\frac{1}{e}\frac{de}{dt} = -0.0739\frac{M_s M_r}{M_p^2}\left(\frac{a}{|a - r|}\right)^5\Omega. \tag{31}$$

Applications of these results are presented in §§ V and VI. Here we merely note that the satellite is repelled by the ring and its orbital eccentricity is damped. The latter conclusion is dependent on the assumption that the resonances are not saturated (cf. § V*e*).

III. INTERACTIONS DURING A CLOSE ENCOUNTER

In this section we rederive equations (28) and (29) without reference to individual resonances. This alternate derivation helps to clarify the mechanisms of angular momentum transport between a satellite and a differentially rotating disk. The approximation we use here was applied previously by Julian and Toomre (1966) and by Lin and Papaloizou (1979). It was originally devised by Hill for his lunar theory.

a) Basic Model

We introduce a local coordinate system with origin at $r = R$ which revolves with $\Omega = \Omega(R)$. The x axis points radially outward, and the y axis points in the direction of increasing θ. For $x/R \ll 1$ and $y/R \ll 1$, the equations of motion of a particle of mass m subject to a central potential $\Phi(r)$ and a perturbation potential ϕ_p read (Spitzer and Schwarzschild 1953)

$$\ddot{x} + 4\Omega A x - 2\Omega\dot{y} = -\partial\phi_p/\partial x, \tag{32}$$

$$\ddot{y} + 2\Omega\dot{x} = -\partial\phi_p/\partial y, \tag{33}$$

where $A \equiv A(R)$. The unperturbed ($\phi_p = 0$) motion of a particle is given by

$$x = \alpha - \epsilon\cos(\kappa t + \delta), \qquad y = 2A\alpha t + \gamma + \frac{2\Omega}{\kappa}\epsilon\sin(\kappa t + \delta). \tag{34}$$

Here α, ϵ, γ, and δ are constants and $\kappa = \kappa(R)$.

The equations of motion have an "energy" integral if $\partial\phi_p/\partial t = 0$ and an "angular momentum" integral if $\partial\phi_p/\partial y = 0$:

$$E = \frac{M}{2}\left[\left(\frac{dx}{dt}\right)^2 + \left(\frac{dy}{dt}\right)^2 + 4\Omega A x^2\right] + M\phi_p\,, \qquad H = M[dy/dt + 2\Omega x]\,. \tag{35}$$

From equations (34) and (35), we see that the energy and angular momentum of an unperturbed particle may be expressed as

$$E = M\frac{\kappa^2}{2}[\epsilon^2 + (A/\Omega)\alpha^2]\,, \tag{36}$$

$$H = 2MB\alpha\,. \tag{37}$$

The equations which govern the evolution of the osculating orbital elements are obtained by applying the method of variation of constants to equations (32)–(34). We find

$$\frac{d\alpha}{dt} = -\frac{1}{2B}\frac{\partial\phi_p}{\partial\gamma}\,, \qquad \frac{d\gamma}{dt} = \frac{1}{2B}\frac{\partial\phi_p}{\partial\alpha}\,, \qquad \frac{d\epsilon}{dt} = -\frac{1}{\kappa\epsilon}\frac{\partial\phi_p}{\partial\delta}\,, \qquad \frac{d\delta}{dt} = \frac{1}{\kappa\epsilon}\frac{\partial\phi_p}{\partial\epsilon}\,. \tag{38}$$

It is often convenient to replace ϵ and δ by the auxiliary variables $h \equiv \epsilon \sin\delta$ and $k \equiv \epsilon\cos\delta$ which satisfy

$$\frac{dh}{dt} = \frac{1}{\kappa}\frac{\partial\phi_p}{\partial k}\,, \qquad \frac{dk}{dt} = -\frac{1}{\kappa}\frac{\partial\Phi_p}{\partial h}\,. \tag{39}$$

For later comparison with the results obtained in § II, we note that α and ϵ are related to a, r, and e by

$$\alpha_s = a - R\,, \tag{40a}$$

$$\alpha_r = r - R\,, \tag{40b}$$

$$\epsilon = eR\,. \tag{40c}$$

b) First and Second Order Perturbations

We consider the changes in α and ϵ produced by a single close encounter of two particles with masses M_r and M_s. The interaction energy is $M_rM_s\phi$, where

$$\phi = -\frac{G}{[(x_s - x_r)^2 + (y_s - y_r)^2]^{1/2}} = -\frac{G}{d}\,. \tag{41}$$

The quantity ϕ may be expressed as a function of α_i, γ_i, h_i, k_i, and t where $i = r, s$. From the manner in which α_i, γ_i, h_i, and k_i enter ϕ, it follows that

$$\frac{\partial\phi}{\partial z_r} = -\frac{\partial\phi}{\partial z_s}\,, \tag{42}$$

where z is any one of these elements. This symmetry does not apply to the elements ϵ and δ. For this reason, we use h and k instead of ϵ and δ in the initial development of the equations for the second order perturbations.

The first order variations, $\delta_1 z_i(t)$, follow directly from equations (38) and (39). From the above symmetries $M_s\delta_1 z_s(t) = -M_r\delta_1 z_r(t)$ for $z = \alpha$, γ, h, and k.

The second order variation of α_s satisfies

$$\frac{d}{dt}\delta_2\alpha_s = -\frac{1}{2B}\sum_{i=r,s}\left\{\frac{\partial^2\phi_s}{\partial\alpha_i\partial\gamma_s}\delta_1\alpha_i + \frac{\partial^2\phi_s}{\partial\gamma_i\partial\gamma_s}\delta_1\gamma_i + \frac{\partial^2\phi_s}{\partial h_i\partial\gamma_s}\delta_1 h_i + \frac{\partial^2\phi_s}{\partial k_i\partial\gamma_s}\delta_1 k_i\right\}. \tag{43}$$

To obtain the total second order change of α_s due to the encounter, $\Delta_2\alpha_s \equiv \delta_2\alpha_s(\infty)$, we integrate equation (43) over $-\infty < t < \infty$ and use the symmetry relations. We obtain

$$\Delta_2\alpha_s = M_r(M_r + M_s)\left\{\frac{1}{4B^2}\left[\int_{-\infty}^{\infty} dt\,\frac{\partial^2\phi}{\partial\alpha_s\partial\gamma_s}\int_{-\infty}^{t} dt'\,\frac{\partial\phi}{\partial\gamma_s} - \int_{-\infty}^{\infty} dt\,\frac{\partial^2\phi}{\partial\gamma_s^2}\int_{-\infty}^{t} dt'\,\frac{\partial\phi}{\partial\alpha_s}\right]\right.$$
$$\left. + \frac{1}{2B\kappa}\left[-\int_{-\infty}^{\infty} dt\,\frac{\partial^2\phi}{\partial h_s\partial\gamma_s}\int_{-\infty}^{t} dt'\,\frac{\partial\phi}{\partial k_s} + \int_{-\infty}^{\infty} dt\,\frac{\partial^2\phi}{\partial k_s\partial\gamma_s}\int_{-\infty}^{t} dt'\,\frac{\partial\phi}{\partial h_s}\right]\right\}. \tag{44}$$

The second order variation of ϵ is related to the first and second order variations of h and k by

$$\delta_2\epsilon = \frac{h\delta_2 h + k\delta_2 k}{(h^2+k^2)^{1/2}} + \frac{(k\delta_1 h - h\delta_1 k)^2}{2(h^2+k^2)^{3/2}}. \tag{45}$$

A derivation analogous to that leading to equation (44) yields

$$\Delta_1 h_s = \frac{M_r}{\kappa}\int_{-\infty}^{\infty} dt\,\frac{\partial\phi}{\partial k_s}, \tag{46}$$

$$\Delta_2 h_s = M_r(M_r+M_s)\left\{\frac{1}{2B\kappa}\left[-\int_{-\infty}^{\infty} dt\,\frac{\partial^2\phi}{\partial\alpha_s\partial k_s}\int_{-\infty}^{t} dt'\,\frac{\partial\phi}{\partial\gamma_s} + \int_{-\infty}^{\infty} dt\,\frac{\partial^2\phi}{\partial\gamma_s\partial k_s}\int_{-\infty}^{t} dt'\,\frac{\partial\phi}{\partial\alpha_s}\right]\right.$$
$$\left. + \frac{1}{\kappa^2}\left[\int_{-\infty}^{\infty} dt\,\frac{\partial^2\phi}{\partial h_s\partial k_s}\int_{-\infty}^{t} dt'\,\frac{\partial\phi}{\partial k_s} - \int_{-\infty}^{\infty} dt\,\frac{\partial^2\phi}{\partial k_s^2}\int_{-\infty}^{t} dt'\,\frac{\partial\phi}{\partial h_s}\right]\right\}. \tag{47}$$

The analogous expressions for $\Delta_1 k_s$ and $\Delta_2 k_s$ are obtained by applying the transformation $h_s \to k_s$, $k_s \to -h_s$ to equations (46) and (47).

Next we change from h_s and k_s to ϵ_s and δ_s in the equations for $\Delta_2\alpha_s$ and $\Delta_2\epsilon_s$. This is accomplished by using the relations

$$\frac{\partial}{\partial h} = \sin\delta\,\frac{\partial}{\partial\epsilon} + \frac{\cos\delta}{\epsilon}\,\frac{\partial}{\partial\epsilon}, \qquad \frac{\partial}{\partial k} = \cos\delta\,\frac{\partial}{\partial\epsilon} - \frac{\sin\delta}{\epsilon}\,\frac{\partial}{\partial\epsilon}. \tag{48}$$

The results are

$$\Delta_2\alpha_s = M_r(M_r+M_s)\left\{\frac{1}{4B^2}\left[\int_{-\infty}^{\infty} dt\,\frac{\partial^2\phi}{\partial\alpha_s\partial\gamma_s}\int_{-\infty}^{t} dt'\,\frac{\partial\phi}{\partial\gamma_s} - \int_{-\infty}^{\infty} dt'\,\frac{\partial^2\phi}{\partial\gamma_s^2}\int_{-\infty}^{t} dt'\,\frac{\partial\phi}{\partial\alpha_s}\right]\right.$$
$$\left. + \frac{1}{2B\kappa\epsilon_s}\left[\int_{-\infty}^{\infty} dt\,\frac{\partial^2\phi}{\partial\epsilon_s\partial\gamma_s}\int_{-\infty}^{t} dt'\,\frac{\partial\phi}{\partial\delta_s} - \int_{-\infty}^{\infty} dt\,\frac{\partial^2\phi}{\partial\delta_s\partial\gamma_s}\int_{-\infty}^{t} dt'\,\frac{\partial\phi}{\partial\epsilon_s}\right]\right\} \tag{49}$$

and

$$\epsilon_s\Delta_2\epsilon_s = M_r(M_r+M_s)\left\{\frac{1}{2B\kappa}\left[\int_{-\infty}^{\infty} dt\,\frac{\partial^2\phi}{\partial\alpha_s\partial\delta_s}\int_{-\infty}^{t} dt'\,\frac{\partial\phi}{\partial\gamma_s} - \int_{-\infty}^{\infty} dt\,\frac{\partial^2\phi}{\partial\gamma_s\partial\delta_s}\int_{-\infty}^{t} dt'\,\frac{\partial\phi}{\partial\alpha_s}\right]\right.$$
$$+ \frac{1}{\kappa^2\epsilon_s}\left[\int_{-\infty}^{\infty} dt\,\frac{\partial^2\phi}{\partial\delta_s\partial\epsilon_s}\int_{-\infty}^{t} dt'\,\frac{\partial\phi}{\partial\delta_s} - \int_{-\infty}^{\infty} dt\,\frac{\partial^2\phi}{\partial\delta_s^2}\int_{-\infty}^{t} dt'\,\frac{\partial\phi}{\partial\epsilon_s}\right]$$
$$\left. - \frac{1}{2}\left(\frac{1}{\kappa}\int_{-\infty}^{\infty} dt\,\frac{\partial\phi}{\partial\epsilon_s}\right)^2 - \frac{1}{2}\left(\frac{1}{\kappa\epsilon_s}\int_{-\infty}^{\infty} dt\,\frac{\partial\phi}{\partial\delta_s}\right)^2\right\} + \frac{M_r^2}{2}\left(\frac{1}{\kappa}\int_{-\infty}^{\infty} dt\,\frac{\partial\phi}{\partial\epsilon_s}\right)^2. \tag{50}$$

The piece proportional to M_r^2 in $\epsilon_s\Delta_2\epsilon_s$ arises from the term in equation (45) which is quadratic in the first order variations of h_s and k_s.

Equations (49) and (50) describe the second order changes in α_s and ϵ_s produced by a close encounter of masses M_r and M_s. However, our aim is to determine the changes in α_s and ϵ_s due to the interaction of a continuous ring of small particles of total mass M_r with a satellite of mass M_s. In this case, the terms proportional to M_s^2 account for successive first order perturbations of the satellite by different particles of the circular ring. Since the potential of a circular ring may be absorbed into the unperturbed potential, these terms do not contribute to $\Delta_2\alpha_s$ and $\Delta_2\epsilon_s$. (A formal proof of this result may be constructed but is not given here.) In the terms proportional to M_sM_r, M_r should be replaced by $M_r d\gamma_r/2\pi r$ and the resulting expression integrated over $0 \le \gamma_r \le 2\pi r$.

To further simplify the equations for $\Delta_2\alpha_s$ and $\Delta_2\epsilon_s$, we make use of the relations

$$\partial\phi/\partial\gamma_r = -\partial\phi/\partial\gamma_s \tag{51}$$

and

$$\frac{\partial\phi}{\partial t} = \kappa\frac{\partial\phi}{\partial\delta_s} + 2A(\alpha_s-\alpha_r)\frac{\partial\phi}{\partial\gamma_s}. \tag{52}$$

Equation (51) is a special case of equation (42) with γ substituted for z. Equation (52) follows immediately from the form of ϕ as given by equations (34) and (41) and the fact that $\epsilon_r = 0$.

To simplify $\Delta_2\alpha_s$, we apply equation (51) to the second term in each of the square brackets of equation (49). Next, we integrate by parts with respect to γ_r and then change the order of the integrations over t and t'. After applying equation (51) again, the two terms in each square bracket combine to yield the product of two one-dimensional integrals.

The prescription for simplifying $\Delta_2\epsilon_s$ is similar to that used for $\Delta_2\alpha_s$. However, in this case equation (52) is applied first to express $\partial\phi/\partial\delta_s$ in terms of $\partial\phi/\partial\gamma_s$ and $\partial\phi/\partial t$. The integrations by parts and the interchanges of order of the integrations over time now follow the procedure outlined for $\Delta_2\alpha_s$. After $\Delta_2\epsilon_s$ has been expressed as the sum of terms each involving the product of two one-dimensional integrals, equation (52) is applied again to express $\partial\phi/\partial\gamma_s$ in terms of $\partial\phi/\partial\delta_s$.

The simplified versions of $\Delta_2\alpha_s$ and $\Delta_2\epsilon_s$ read

$$\Delta_2\alpha_s = \frac{M_s M_r}{2\pi r}\int_0^{2\pi r} d\gamma_r \left\{ \frac{1}{4B^2}\int_{-\infty}^{\infty} dt\,\frac{\partial^2\phi}{\partial\alpha_s\partial\gamma_s}\int_{-\infty}^{\infty} dt\,\frac{\partial\phi}{\partial\gamma_s} + \frac{1}{2B\kappa\epsilon_s}\int_{-\infty}^{\infty} dt\,\frac{\partial^2\phi}{\partial\epsilon_s\partial\gamma_s}\int_{-\infty}^{\infty} dt\,\frac{\partial\phi}{\partial\delta_s}\right\}, \tag{53}$$

$$\epsilon_s\Delta_2\epsilon_s = \frac{M_s M_r}{2\pi r}\int_0^{2\pi r} d\gamma_r \left\{ \frac{1}{2B\kappa}\int_{-\infty}^{\infty} dt\,\frac{\partial^2\phi}{\partial\alpha_s\partial\delta_s}\int_{-\infty}^{\infty} dt\,\frac{\partial\phi}{\partial\gamma_s} + \frac{1}{\kappa^2\epsilon_s}\int_{-\infty}^{\infty} dt\,\frac{\partial^2\phi}{\partial\delta_s\partial\epsilon_s}\int_{-\infty}^{\infty} dt\,\frac{\partial\phi}{\partial\delta_s} - \frac{1}{2}\left(\frac{1}{\kappa}\int_{-\infty}^{\infty} dt\,\frac{\partial\Phi}{\partial\epsilon_s}\right)^2 - \frac{1}{2}\left(\frac{1}{\kappa\epsilon_s}\int_{-\infty}^{\infty} dt\,\frac{\partial\phi}{\partial\delta_s}\right)^2\right\}. \tag{54}$$

In writing equations (53) and (54), we have discarded some boundary terms which arise from the integrations by parts over γ_r. These terms are smaller than those retained by order $|\alpha_s - \alpha_r|/R \ll 1$.

We proceed to evaluate $\Delta_2\alpha_s$ and $\Delta_2\epsilon_s$ to lowest order in ϵ_s. We start by expanding ϕ in a Taylor series in ϵ_s using the identity

$$\frac{\partial\phi}{\partial\epsilon_s} = -\cos u\,\frac{\partial\phi}{\partial x_s} + \frac{2\Omega}{\kappa}\sin u\,\frac{\partial\phi}{\partial y_s}, \tag{55}$$

where $u \equiv \kappa t + \delta_s$. We also need the second and third order derivatives which read

$$\frac{\partial^2\phi}{\partial\epsilon_s^2} = \frac{(1+\cos 2u)}{2}\frac{\partial^2\phi}{\partial x_s^2} + \left(\frac{2\Omega}{\kappa}\right)^2\frac{(1-\cos 2u)}{2}\frac{\partial^2\phi}{\partial y_s^2} - \frac{2\Omega}{\kappa}\sin 2u\,\frac{\partial^2\phi}{\partial x_s\partial y_s}, \tag{56}$$

$$\frac{\partial^3\phi}{\partial\epsilon_s^3} = -\frac{(3\cos u + \cos 3u)}{4}\frac{\partial^3\phi}{\partial x_s^3} + 2\left(\frac{\Omega}{\kappa}\right)^3(3\sin u - \sin 3u)\frac{\partial^3\phi}{\partial y_s^3} + \frac{3\Omega}{2\kappa}(\sin u + \sin 3u)\frac{\partial^3\phi}{\partial x_s^2\partial y_s} - 3\left(\frac{\Omega}{\kappa}\right)^2(\cos u - \cos 3u)\frac{\partial^3\phi}{\partial x_s\partial y_s^2}. \tag{57}$$

Next we replace $\partial\phi/\partial\gamma_s$ by $-[2A(\alpha_s - \alpha_r)]^{-1}\kappa\,\partial\phi/\partial\delta_s$ and $(2\pi r)^{-1}\int_0^{2\pi r} d\gamma_r$ by $(2\pi)^{-1}\int_0^{2\pi} d\delta_s$ in equations (53) and (54). The latter substitution is not exact unless $\kappa a_r/(2A|a_s - a_r|)$ is an integer, but the error it introduces is only of order $|\alpha_s - \alpha_r|/R \ll 1$.

To calculate $\Delta_2 a_s$ to lowest order in ϵ_s, only the second term in equation (53) is needed. Using the results of the preceding paragraph, we see that this term is equal to

$$\Delta_2\alpha_s = -\frac{M_s M_r}{2\pi}\int_0^{2\pi} d\delta_s \left\{\frac{1}{8AB(\alpha_s - \alpha_r)\epsilon_s}\frac{\partial}{\partial\epsilon_s}\left[\int_{-\infty}^{\infty} dt\,\frac{\partial\phi}{\partial\delta_s}\right]^2\right\}. \tag{58}$$

To lower order in ϵ_s,

$$\int_{-\infty}^{\infty} dt\,\frac{\partial\phi}{\partial\delta_s} = \epsilon_s\int_{-\infty}^{\infty} dt\left(\sin u\,\frac{\partial\phi}{\partial x_s} + \frac{2\Omega}{\kappa}\cos u\,\frac{\partial\phi}{\partial y_s}\right)_0, \tag{59}$$

where the subscript 0 denotes that the partial derivatives,

$$\frac{\partial\phi}{\partial x_s} = \frac{G(x_s - x_r)}{d^3}, \qquad \frac{\partial\phi}{\partial y_s} = \frac{G(y_s - y_r)}{d^3}, \tag{60}$$

are to be evaluated for circular orbits. Thus, we set $x_i = \alpha_i$ and $y_i = 2A\alpha_i t + \gamma_i$ for $i = r, s$. Then we change the

variable of integration from t to $\tau = 2At + (\gamma_s - \gamma_r)/(\alpha_s - \alpha_r)$ and obtain

$$\int_{-\infty}^{\infty} dt \frac{\partial \phi}{\partial \delta_s} = \frac{\epsilon_s G \sin v}{2|A|(\alpha_s - \alpha_r)^2} \int_{-\infty}^{\infty} \frac{d\tau}{(1+\tau^2)^{3/2}} \left[\cos\left(\frac{\kappa\tau}{2|A|}\right) - \frac{2\Omega\tau}{\kappa} \sin\left(\frac{\kappa\tau}{2|A|}\right) \right], \tag{61}$$

where $v \equiv \delta_s - \kappa(\gamma_s - \gamma_r)/[2A(\alpha_s - \alpha_r)]$. Integration over τ yields

$$\int_{-\infty}^{\infty} dt \frac{\partial \phi}{\partial \delta_s} = \frac{\epsilon_s G \kappa \sin v}{2A^2(\alpha_s - \alpha_r)^2} \left[\frac{2\Omega}{\kappa} K_0\left(\frac{\kappa}{2|A|}\right) + K_1\left(\frac{\kappa}{2|A|}\right) \right]. \tag{62}$$

Combining equations (58) and (62), we arrive at the final expression for $\Delta_2 \alpha_s$ which reads

$$\Delta_2 \alpha_s = \frac{G^2 M_s M_r \kappa^2}{32|A|^5 B(\alpha_s - \alpha_r)^5} \left[\frac{2\Omega}{\kappa} K_0\left(\frac{\kappa}{2|A|}\right) + K_1\left(\frac{\kappa}{2|A|}\right) \right]^2. \tag{63}$$

To obtain da/dt from $\Delta_2 \alpha_s$, we use equation (40) and the fact that the entire ring passes by the satellite in a time

$$\Delta t = \frac{\pi a}{|A(a-r)|}. \tag{64}$$

Thus

$$\frac{da}{dt} = \operatorname{sgn}(a-r) \frac{\Omega G^2 M_s M_r}{8\pi A^4 a (a-r)^4} [(2\Omega/\kappa) K_0(\kappa/2|A|) + K_1(\kappa/2|A|)]^2. \tag{65}$$

In writing da/dt we have set $\kappa^2 = 4\Omega B$. Note that equation (65) for da/dt is identical to equation (28) obtained by summing the torques at discrete resonances.

The calculation of $\Delta_2 \epsilon_s$ proceeds along similar lines to that of $\Delta_2 \alpha_s$. Each of the four terms in equation (54) makes a contribution of order ϵ_s to $\Delta_2 \epsilon_s$. The first of these terms may be written as

$$\Delta_2 \epsilon_s|_1 = \frac{M_s M_r}{16\pi |A| B(\alpha_s - \alpha_r)\epsilon_s} \frac{\partial}{\partial \alpha_s} \int_0^{2\pi} d\delta_s \left(\int_{-\infty}^{\infty} dt \frac{\partial \phi}{\partial \delta_s} \right)^2. \tag{66}$$

With the aid of equation (62), we find

$$\Delta_2 \epsilon_s|_1 = -\frac{G^2 M_s M_r \kappa^2 \epsilon_s}{16|A|^5 B(\alpha_s - \alpha_r)^6} \left[\frac{2\Omega}{\kappa} K_0\left(\frac{\kappa}{2|A|}\right) + K_1\left(\frac{\kappa}{2|A|}\right) \right]^2. \tag{67}$$

The three remaining terms may be grouped as

$$\Delta_2 \epsilon_s|_{2+3+4} = \frac{M_s M_r}{4\pi\kappa^2 \epsilon_s} \int_0^{2\pi} d\delta_s \left\{ \frac{\partial}{\partial \epsilon_s} \left[\frac{1}{\epsilon_s} \left(\int_{-\infty}^{\infty} dt \frac{\partial \phi}{\partial \delta_s} \right)^2 \right] - \left(\int_{-\infty}^{\infty} dt \frac{\partial \phi}{\partial \epsilon_s} \right)^2 \right\}. \tag{68}$$

To calculate $\Delta_2 \epsilon_s$ to first order in ϵ_s, we must expand ϕ to third order in ϵ_s in equation (68). We denote by $\phi^{(n)}$ the nth derivative of ϕ with respect to ϵ_s evaluated at $\epsilon_s = 0$. Then to third order in ϵ_s,

$$\phi = \phi^{(0)} + \phi^{(1)}\epsilon_s + \phi^{(2)}(\epsilon_s^2/2) + \phi^{(3)}(\epsilon_s^3/6). \tag{69}$$

When equation (69) is substituted into equation (68), the terms which result may be sorted according to the order of the derivatives with respect to ϵ_s which appear in the integral factors. Thus the (m, n) terms are proportional to the product of an integral of $\phi^{(m)}$ and an integral of $\phi^{(n)}$. Using this nomenclature, we assert that the $(0, n)$ terms vanish individually, the $(1, 2)$ terms vanish when averaged over δ_s, and the $(1, 1)$ and $(1, 3)$ terms sum to zero when averaged over δ_s. These assertions may be verified by inspection of the forms of equations (55)–(57) and (68). It is not necessary to evaluate the t integrals.

It is now established that to first order in ϵ_s only the $(2, 2)$ terms survive. From equations (56) and (68), we find that these yield

$$\begin{aligned} \Delta_2 \epsilon_s|_{2+3+4} = \frac{M_s M_r \epsilon_s}{16\pi\kappa^2} \int_0^{2\pi} d\delta_s \Bigg\{ 3 \Bigg\langle \int_{-\infty}^{\infty} dt \Bigg[\sin 2u \left(\frac{\partial^2 \phi}{\partial x_s^2} - \left(\frac{2\Omega}{\kappa}\right)^2 \frac{\partial^2 \phi}{\partial y_s^2} \right) + \frac{4\Omega}{\kappa} \cos 2u \frac{\partial^2 \phi}{\partial x_s \partial y_s} \Bigg]_0 \Bigg\rangle^2 \\ - \Bigg\langle \int_{-\infty}^{\infty} dt \Bigg[(1 + \cos 2u) \frac{\partial^2 \phi}{\partial x_s^2} + \left(\frac{2\Omega}{\kappa}\right)^2 (1 - \cos 2u) \frac{\partial^2 \phi}{\partial y_s^2} \\ - \frac{4\Omega}{\kappa} \sin 2u \frac{\partial^2 \phi}{\partial x_s \partial y_s} \Bigg]_0 \Bigg\rangle^2 \Bigg\}, \end{aligned} \tag{70}$$

where

$$\frac{\partial^2\phi}{\partial x_s^2} = -\frac{G[2(x_s - x_r)^2 - (y_s - y_r)^2]}{d^5},$$
$$\frac{\partial^2\phi}{\partial y_s^2} = -\frac{G[2(y_s - y_r)^2 - (x_s - x_r)^2]}{d^5},$$
$$\frac{\partial^2\phi}{\partial x_s \partial y_s} = -3G\frac{(x_s - x_r)(y_s - y_r)}{d^5}. \tag{71}$$

Equations (70) and (71) reduce to

$$\Delta_2\epsilon_s|_{2+3+4} = \frac{G^2 M_s M_r \epsilon_s}{32A^2\kappa^2(\alpha_s - \alpha_r)^6}\left\{\left\langle\int_{-\infty}^{\infty} d\tau\left[\cos\left(\frac{\kappa\tau}{|A|}\right)\left(\frac{8\Omega^2 + \kappa^2}{\kappa^2(1+\tau^2)^{3/2}} - \frac{3(4\Omega^2+\kappa^2)}{\kappa^2(1+\tau^2)^{5/2}}\right)\right.\right.\right.$$
$$\left.\left.\left. - \sin\left(\frac{\kappa\tau}{|A|}\right)\left(\frac{12\Omega\tau}{\kappa(1+\tau^2)^{5/2}}\right)\right]\right\rangle^2$$
$$\left. - \left\langle\int_{-\infty}^{\infty} d\tau\left[\frac{8\Omega^2 - \kappa^2}{\kappa^2(1+\tau^2)^{3/2}} - \frac{3(4\Omega^2-\kappa^2)}{\kappa^2(1+\tau^2)^{5/2}}\right]\right\rangle^2\right\}. \tag{72}$$

The integrals in equation (72) which involve trigonometric functions may be expressed in terms of modified Bessel functions. The other integrals are elementary. We find

$$\Delta_2\epsilon_s|_{2+3+4} = \frac{\kappa^2 G^2 M_s M_r \epsilon_s}{A^6(\alpha_s - \alpha_r)^6}\left\{\langle[1 + (2\Omega/\kappa)^2]K_0(\kappa/|A|) + [|A|/\kappa + 4\Omega/\kappa]K_1(\kappa/|A|)\rangle^2 - \left(\frac{A}{\kappa}\right)^4\right\}. \tag{73}$$

To determine de/dt we combine equations (40), (64), (67), and (73) which yield

$$\frac{1}{e}\frac{de}{dt} = \frac{\kappa^2 G^2 M_s M_r}{8\pi|A|^5 a|a-r|^5}\left\{\langle[1 + (2\Omega/\kappa)^2]K_0(\kappa/|A|) + [|A|/\kappa + 4\Omega/\kappa]K_1(\kappa/|A|)\rangle^2\right.$$
$$\left. - \frac{|A|}{2B}\langle(2\Omega/\kappa)K_0(\kappa/2|A|) + K_1(\kappa/2|A|)\rangle^2 - \left(\frac{A}{\kappa}\right)^4\right\}. \tag{74}$$

Note that $d \ln a/dt$ is smaller than $d \ln e/dt$ by a factor $|a - r|/a$ and has been neglected. A comparison of equations (29) and (74) reveals that the close encounter approximation duplicates the expression for de/dt that we obtained by summing the torques at discrete resonances except for the addition of a term proportional to $(A/\kappa)^4$. The origin of the "extra term" is explained below.

c) *Eccentricity Driving*

A satellite moving on an eccentric orbit forces an eccentricity in an initially circular ring. The potential components responsible for the forced eccentricity have $m = 0$ and $l = \pm 1$. From equations (5)–(10), we see that for $|a - r| \ll a$ the dominant terms in the forcing potential are

$$V(r) = (\phi^s_{1,0} + \phi^s_{-1,0})\cos\kappa t \approx -\frac{GM_s e}{\pi|a-r|}\cos\kappa t. \tag{75}$$

The forced response of a ring particle is obtained by substituting V for ϕ_p in equation (33). To first order in M_s we find

$$x(t) = \frac{GM_s e \operatorname{sgn}(a-r) t \sin\kappa t}{2\pi\kappa(a-r)^2}, \tag{76}$$

subject to the initial conditions $x(0) = \dot{x}(0) = \dot{y}(0) = 0$. In deriving equation (76), we have set $\kappa_s = \kappa_L = \kappa$ since κ has been treated as a constant in this section. More generally, equation (76) is valid for $|\kappa_s - \kappa_r|t \ll 1$. For $\kappa t \gg 1$, the ring perturbation is well described as a growing forced eccentricity e_r where

$$e_r = \frac{GM_s e t}{2\pi\kappa a(a-r)^2}. \tag{77}$$

As the ring's eccentricity grows, the satellite's eccentricity e diminishes. To relate the changes in e_r and e, we use the

conservation laws (cf. eqs. [36] and [37]) and the fact that the circularly symmetric potential V does not transfer angular momentum between the satellite and the ring. Thus

$$\Delta e^2 = -\frac{M_r}{M_s}\Delta e_r^2 \cdot \tag{78}$$

With e_r evaluated for $t = \Delta t$, the time interval between successive passages of the satellite past a given ring particle (cf. eq. [64]),

$$\Delta e = -\frac{G^2 M_s M_r e}{8\kappa^2 A^2 (a-r)^6} \cdot \tag{79}$$

This is just the value of the "extra term" in Δe obtained in the close encounter approximation (cf. eq. [73]).

It is clear that the "extra term" in de/dt does not arise from a true resonance and does not represent a secular change in e. Its appearance in the close encounter derivation of de/dt is an artifact of this approximation's limited frequency resolution which does not enable us to distinguish between a long period term and a secular one.

IV. TORQUE CUTOFF

We have shown that the torque density at radius r due to a satellite moving on a circular orbit of radius a is proportional to sgn $(r-a)(a-r)^{-4}$ for $c/\Omega \ll |a-r| \ll a$ (cf. eq. [18]). If the satellite orbits within a disk, we are unable to find the total torque since equation (18) fails in the region $|a-r| \lesssim c/\Omega$ where the torque density is greatest. Our purpose in this section is to derive formulae for the total torques exerted by the satellite on the parts of the disk interior and exterior to it. For simplicity, we consider gaseous disks. They are the subject of our astronomical application in § VI. Results for disks composed of discrete particles should be similar.

We adopt the local Cartesian approximation of § III. The satellite is located at the coordinate origin and gives rise to the time-independent potential $M_s\phi = -GM_s/(x^2+y^2)^{1/2}$. The steady-state response of the disk may be obtained from the hydrodynamic equations developed in Goldreich and Lynden-Bell (1965) and GT2. The unperturbed surface density Σ and the sound speed c are assumed to be constant. We denote the perturbed surface density by σ. The relevant equations are

$$\begin{Bmatrix}\sigma\\ \phi\end{Bmatrix}(x,y) = \mathrm{Re}\int_0^\infty dk_y \exp(ik_y y)\begin{Bmatrix}\hat{\sigma}\\ \hat{\phi}\end{Bmatrix}(k_y, x)\,, \tag{80}$$

$$\hat{\sigma}(k_y,\tau) = k_y\Sigma\int_{-\infty}^{\infty} d\tau\tilde{\theta}(k_y,\tau)\exp(ik_y\tau x)\,, \tag{81}$$

$$\tilde{\phi}(k_y,\tau) = \frac{1}{2\pi}\int_{-\infty}^{\infty} dx\hat{\phi}(k_y,x)\exp(-ik_y\tau x) = -\frac{G}{\pi k_y(1+\tau^2)^{1/2}}\,, \tag{82}$$

$$\frac{d^2\tilde{\theta}}{d\tau^2} - \frac{2\tau}{(1+\tau^2)}\frac{d\tilde{\theta}}{d\tau} + \left[\frac{2B}{A(1+\tau^2)} + \frac{\kappa^2}{4A^2} - \frac{\kappa k_y c}{2A^2 Q}(1+\tau^2)^{1/2} + \frac{k_y^2 c^2}{4A^2}(1+\tau^2)\right]\tilde{\theta} = -\frac{M_s k_y^2}{4A^2}\tilde{\phi}(k_y,\tau)(1+\tau^2)\,. \tag{83}$$

Note that our sign conventions for A and Ω differ from GT2; as a result some of our equations differ slightly from their analogs there. Equation (83) (GT2, eq. [34]) is to be solved subject to the boundary conditions $\tilde{\theta}$, $d\tilde{\theta}/d\tau \to 0$ as $\tau \to \infty$;

$$Q \equiv \kappa c/\pi G\Sigma \tag{84}$$

is the Toomre (1964) stability parameter. The disk is stable to axisymmetric perturbations if and only if $Q \geq 1$. We consider only stable disks.

To determine the torque exerted on the disk, we compute the angular momentum flux through the disk in the limit $|x| \to \infty$. This is a valid procedure because we are dealing with a stationary state and all of the angular momentum which is deposited in the disk is transported toward $\tilde{\theta}x = \pm\infty$ by density waves. As $|x| \to \infty$, the factor $\exp(ik_y\tau x)$ in the integrand of equation (81) oscillates rapidly. Thus the main contribution to $\hat{\sigma}(k_y, x)$ comes from large values of τ where $\tilde{\theta}(\tau)$ also oscillates rapidly and there is a point of stationary phase. At large τ, the WKB solutions of differential equation (83) have the form

$$\tilde{\theta}(k_y,\tau) = S_+\tau^{1/2}\exp\left(\frac{ik_y c\tau^2}{4|A|}\right) + S_-\tau^{1/2}\exp\left(-\frac{ik_y c\tau^2}{4|A|}\right). \tag{85}$$

The amplitudes $S_\pm$ are obtained by numerical integration of equation (83).[1] Because equation (83) is real, $S_+^* = S_-$.

[1] For $Q^{-1} = 0$ the differential equation may be solved analytically. The solutions contain parabolic cylinder functions.

Substituting equation (85) into equation (81) and applying the method of stationary phase, we find

$$\hat{\sigma}(k_y, x) = \frac{2|A|\Sigma}{c} S_{\mp}(2\pi k_y|x|)^{1/2} \exp\left(\pm\frac{ik_y|A|x^2}{c} \mp \frac{i\pi}{4}\right) \qquad \text{as } x \to \pm\infty . \tag{86}$$

These solutions are trailing spiral wave trains.

Spiral density waves transport angular momentum by gravitational torques and by advective transport (Lynden-Bell and Kalnajs 1972, GT3). In regions far from corotation ($|x| \to \infty$), advective transport is dominant. To derive the appropriate expression for the advective angular momentum flux in local Cartesian coordinates, we make a slight modification of the development in § II of GT3 and obtain

$$F_H = 4\pi^2 Rc|A|\Sigma \int_0^\infty k_y |S_\pm|^2 dk_y . \tag{87}$$

To adapt this relation to a circularly symmetric disk, we replace $k_y R$ by the azimuthal wavenumber m. A single value of m corresponds to an interval $dk_y = 1/R$. Thus,

$$F_H = \sum_{m=1}^{\infty} F_H(m) ,$$

where

$$F_H(m) = 4\pi^2 c|A|\Sigma m|S_\pm|^2/R , \qquad m \gg 1 . \tag{88}$$

In the limit $m = k_y R \ll \Omega R/c$, the WKB approximation enables us to solve equation (83) analytically (cf. GT2, eqs. [36] and [46]). For

$$\frac{Q^2 - 1}{Q^2} \gg \frac{4mc|A|}{\kappa^2 R} \tag{89}$$

we obtain

$$|S_\pm^{\rm WKB}| = \frac{GM_s}{2\pi|A|}\left(\frac{m}{c\kappa R}\right)^{1/2} \{(2\Omega/\kappa)K_0(\kappa/2|A|) + K_1(\kappa/2|A|)\} . \tag{90}$$

If inequality (89) is not satisfied, the density waves tunnel through the forbidden region around corotation and are amplified (Mark 1976; GT2). As a result, there is interference between density waves which originate on opposite sides of corotation and $F_H(m)$ oscillates rapidly witn m. The WKB approximation may also be applied to solve equation (83) in this limit with the aid of appropriate connection formulae. However, we do not include these solutions here.

The angular momentum flux which corresponds to $S_\pm$ given by equation (90) is

$$F_H^{\rm WKB}(m) = \frac{m^2\Sigma}{\kappa|A|}\left(\frac{GM_s}{R}\right)^2 \{(2\Omega/\kappa)K_0(\kappa/2|A|) + K_1(\kappa/2|A|)\}^2 . \tag{91}$$

The torque which excites each density wave train is exerted in the vicinity of a Lindblad resonance at $r - a = \pm\kappa a/(2|A|m)$ (see Fig. 1). It is a simple matter to compute the torque density from $F_H^{\rm WKB}(m)$ and to recover equation (18).

To determine the total torque, we must include values of $m \gtrsim \Omega R/c$. We determine $|S_\pm|$ by numerical integration of equation (83) and express the results in terms of the ratio $F_H(m)/F_H^{\rm WKB}(m)$. For a given rotation law, this ratio depends only on Q and $\mu \equiv mc/\Omega R$. The results are plotted in Figure 2 for Keplerian disks with $Q = 2$ and $Q = \infty$.

The total flux may be written as

$$F_H = (GM_s)^2 \frac{\Sigma\Omega^3 R}{\kappa|A|c^3}\{(2\Omega/\kappa)K_0(\kappa/2|A|) + K_1(\kappa/2|A|)\}^2 \int_0^\infty d\mu\, \mu^2 \frac{F_H(m)}{F_H^{\rm WKB}(m)} . \tag{92}$$

The behavior of the integrand is displayed in Figure 3. If we define $\mu_{\rm max}$ by

$$\tfrac{1}{3}\mu_{\rm max}^3 = \int_0^\infty d\mu\, \mu^2 \frac{F_H(m)}{F_H^{\rm WKB}(m)} , \tag{93}$$

then $\mu_{\rm max} = 1.45$ for $Q = 2$ and $\mu_{\rm max} = 0.69$ for $Q = \infty$.

A satellite which moves on a circular orbit exerts a torque equal to $\mp F_H$ on the parts of the disk which are interior and exterior to its orbit. We apply this result to a simple problem in § VI.

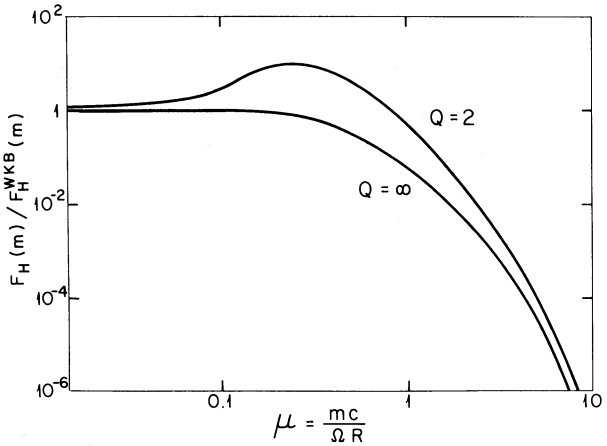

FIG. 2.—The ratio of the actual angular momentum flux from a resonance to the flux calculated from a WKB approximation (eq. [91]). The azimuthal wavenumber m is assumed to be $\gg 1$. Q denotes Toomre's stability parameter (eq. [84]).

V. EXTENSIONS AND REFINEMENTS

Here we discuss some details of the application of our results to planetary rings. Out of necessity we settle for order-of-magnitude calculations. To simplify matters we specialize to circular satellite orbits and Keplerian disks.

We consider both gaseous and particulate disks. The latter are assumed to be composed of particles of radius b and density ρ which possess random velocities of order c. The normal optical depth τ, the collision frequency ω_c, and kinematic viscosity ν satisfy

$$\tau \approx \Sigma/b\rho\,, \tag{94}$$

$$\omega_c \approx \Omega\tau\,, \tag{95}$$

$$\nu \approx \frac{c^2\tau}{\Omega(1+\tau^2)}\,, \tag{96}$$

(Goldreich and Tremaine 1978*a*). The significance of the disk's self-gravity for local dynamics is measured by Toomre's parameter Q (eq. [84]). A disk is self-gravitating in the vertical direction if $Q = O(1)$.

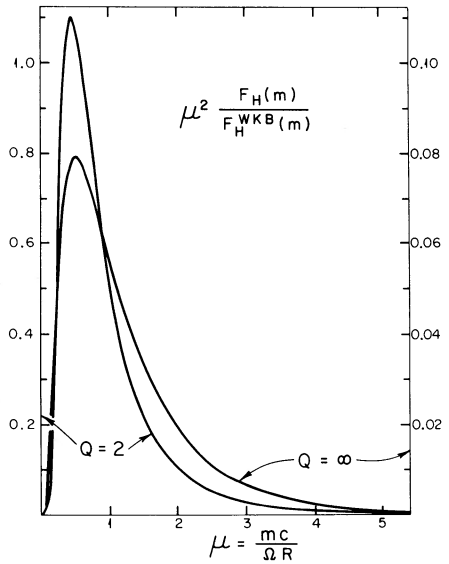

FIG. 3.—Plot of the integrand of eq. (92). The area under each curve is proportional to the total angular momentum flux excited in the disk by a circular satellite. Note that the vertical scales for the two curves are different.

a) Angular Momentum Deposition

We inquire about the fate of the angular momentum (positive or negative) which is deposited at a Lindblad resonance by an external torque. For disks composed of gas, the angular momentum is carried away from the resonance by a trailing density wave (GT1; GT2; GT3). The angular momentum carried by the wave is transferred to the gas as the wave damps. The viscous damping length l_V satisfies

$$\frac{l_V}{r} \approx \left(\frac{c^3}{Q^3 m^2 v r \Omega^2}\right)^{1/3} \qquad \text{for } Q = O(1)\,,$$

$$\frac{l_V}{r} \approx \left(\frac{c^3}{m^{1/2} v r \Omega^2}\right)^{2/3} \qquad \text{for } Q \gg 1 \tag{97}$$

(GT1). The viscous damping time is obtained from l_V and the group velocity c_g (GT1). We find

$$t_V \approx \Omega^{-1}(\Omega r^2/m^2 v)^{1/3}\,. \tag{98}$$

The viscous damping time is independent of Q because it is determined by the rate at which the perturbed velocity field is sheared by differential rotation. Note that for sufficiently strong perturbations, nonlinear damping will reduce l_V and t_V below the values given here.

The spatial variation of the angular momentum transferred to the disk material is smooth if and only if the damping length is long compared to the distance between adjacent Lindblad resonances, $d_m \approx r/m^2$. If linear viscous damping dominates, this requires

$$m \gg (Q^3 v r \Omega^2/c^3)^{1/4} \qquad \text{for } Q = O(1)\,,$$

$$m \gg (v r \Omega^2/c^3)^{2/5} \qquad \text{for } Q \gg 1\,. \tag{99}$$

The behavior of particulate disks is slightly more complicated. A particulate disk can support sound waves if $\tau \gg 1$ and/or gravity waves if $Q = O(1)$. In these cases equation (97) for the damping length is valid, with the viscosity given by equation (96). Note that for $Q \gg 1$ the radial interval Δr_1 occupied by the first cycle of the wave is given by (cf. GT1)

$$\frac{\Delta r_1}{r} \approx \left(\frac{3\pi^2 c^2}{m r^2 \Omega^2}\right)^{1/3}. \tag{100}$$

For a particulate disk with $\tau \gg 1$ the ratio of l_V to Δr_1 is simply

$$l_V/\Delta r_1 \sim (3\pi^2/\tau^2)^{1/3}\,. \tag{101}$$

The concept of a wave is valid only if $\tau \gg 1$ (i.e., if the damping length is longer than the first wavelength).

b) Gap Formation

The radial distribution of the disk material adjusts in response to the addition or subtraction of angular momentum. If the spatial scale of angular momentum deposition is small compared with the spacing between resonances, there will be a tendency for gaps to form at each resonance (GT1). Since the external torque at a Lindblad resonance is proportional to Σ (cf. eq. [13]), any reduction in Σ is accompanied by a reduction of the torque.

The angular momentum ΔH needed to open a gap of radius Δr is $\Delta H \approx \Sigma\Omega(r\Delta r)^2$. The torque

$$T^{\rm L}_{m,m} \approx m^2 r^4 \Omega^2 \Sigma (M_s/M_p)^2 \tag{102}$$

(cf. eq. [13]) supplies ΔH in a time $\Delta t_{\rm open} \approx \Delta H/T^{\rm L}_{m,m}$. The tendency for gap formation is opposed by viscous diffusion which fills up a gap of width Δr on a time scale $\Delta t_{\rm close} \approx (\Delta r)^2/v$. Gap formation requires $\Delta t_{\rm close} > \Delta t_{\rm open}$ or

$$\frac{M_s}{M_p} \gtrsim \frac{1}{m}\left(\frac{v}{\Omega r^2}\right)^{1/2} \qquad \text{or} \qquad \frac{M_s}{M_p} \gtrsim \frac{1}{m}\left(\frac{c}{\Omega r}\right)\left(\frac{\tau}{1+\tau^2}\right)^{1/2} \tag{103}$$

for particulate disks. Note that the requirement for gap formation is independent of Σ. It is also independent of Δr so long as Δr exceeds the viscous damping length.

c) Disks of Low Optical Depth

We consider a particulate disk of low optical depth with $Q \gg 1$. Particle collisions are assumed to be sufficiently inelastic that, far from resonances, the rms random velocity is of order $b\Omega$ (Brahic 1977). The character of the

motion of a particle close to a Lindblad resonance depends on $\Delta a \equiv a - r_{\rm res}$, $\mu \equiv M_s/M_p$, m, and ω_c. We assume $m \gg 1$, $\mu m^2 \ll 1$, and $\omega_c/\Omega \lesssim \mu^{2/3}m^{4/3}$. We distinguish three separate classes of particles, according to the value of $|\Delta a/a|$. Resonant perturbations do not, in general, shuffle particles from one class to another.

For class 1, $\mu^{1/2} < |\Delta a/a| \ll 1$, collisions tend to relax the orbits toward the stable periodic orbit which at Δa has $e \sim \mu|a/\Delta a|$. The periodic orbits do not intersect. The particles have an rms velocity of order $b\Omega$ relative to the periodic motion.

For class 2, $\mu^{2/3}m^{1/3} < |\Delta a/a| < \mu^{1/2}$, there are stable periodic orbits with $e \sim \mu|a/\Delta a|$. However, neighboring periodic orbits cross so that collisions prevent particles from moving on these orbits. The behavior of class 2 particles is as follows: typical orbital eccentricities are $e \sim \mu|a/\Delta a|$ since the time between collisions, ω_c^{-1}, is much longer than the time $t_2 \sim (\Omega m)^{-1}|a/\Delta a|$, over which the resonant perturbation builds up e. Particles in class 2 are most likely to collide with particles of class 1. If either collision partner ends up in class 2, it will tend to have an e which is below average for its $|\Delta a|$. Resonant perturbations will subsequently increase e to a value appropriate to its $|\Delta a|$ in a time of order t_2.

For class 3, $|\Delta a/a| < \mu^{2/3}m^{1/3}$, resonant perturbations increase e from zero up to an average value $\sim \mu^{1/3}m^{-1/3}$ on a time scale $t_3 \sim \Omega^{-1}\mu^{-2/3}m^{-4/3} \ll \omega_c^{-1}$. Class 3 particles collide most often with those from class 1. A particle which finds itself in class 3 after a collision will almost always have a value of e which is below average. The resonant perturbation will then restore e to the average value $\sim \mu^{1/3}m^{-1/3}$ in a time t_3.

The resonant perturbation must supply energy to a particle to build up its eccentricity after a collision. The energy required to produce an eccentricity e is $\Delta E \sim \frac{1}{2}\,\mathrm{sgn}\,(\Omega_p - \Omega)a^2\Omega^2 m e^2$. Assuming that the surface density of particles is independent of Δa, we find that the total rate at which the resonant perturbation supplies energy to the disk is

$$\frac{dE}{dt} \sim \mathrm{sgn}\,(\Omega_p - \Omega)\Sigma a^4\Omega^2\mu^{4/3}m^{2/3}\omega_c\,. \tag{104}$$

The dominant contribution comes from particles with $|\Delta a/a| \lesssim \mu^{2/3}m^{1/3}$ following a collision. Note that the rate of energy dissipation in collisions is $\sim \mathrm{sgn}\,(\Omega - \Omega_p)m^{-1}$ times the rate given in equation (104). From the Jacobi integral the torque exerted on the disk is

$$T = \Omega_p^{-1}\frac{dE}{dt} \sim \mathrm{sgn}\,(\Omega_p - \Omega)\Sigma a^4\Omega^2\left(\frac{M_s}{M_p}\right)^{4/3} m^{2/3}\left(\frac{\omega_c}{\Omega}\right). \tag{105}$$

This expression for T is valid for $\omega_c/\Omega \lesssim \mu^{2/3}m^{4/3}$, since then the forced eccentricity of a class 3 orbit will regain its full value between collisions. Note that for $\omega_c/\Omega \sim \mu^{2/3}m^{4/3}$, T given by equation (105) is equal to the value used elsewhere in the paper (cf. eqs. [13] and [102]). This result indicates that the expression for $T^{\rm L}_{m,m}$ given by equation (13) is valid for all $\omega_c \gtrsim \Omega\mu^{2/3}m^{4/3}$.

Finally, we relate ω_c to the optical depth τ. A conservative estimate is obtained by using equation (95); in this case the torque equation (13) is valid so long as

$$\tau \gtrsim \tau_{\rm crit} \sim \mu^{2/3}m^{4/3}\,. \tag{106}$$

However, equation (95) does not take into account that the particles which contribute most to the torque have much larger random velocities $\sim \mu^{1/3}m^{-1/3}\Omega r$ than the random velocities $\sim \Omega b$ of the class 1 particles with which they collide. Hence, equation (106) represents a conservative upper limit to the value of $\tau_{\rm crit}$.

Franklin *et al.* (1979) have previously obtained results similar to these in a study of the evolution of asteroid orbits.

d) Applications to Planetary Rings

We have described elsewhere (GT1) the manner in which Mimas clears the Cassini division between Saturn's A and B rings. We have also proposed that the narrow rings of Uranus are confined by torques due to small, as yet undiscovered, satellites which orbit within the ring system (Goldreich and Tremaine 1979*a*). It seems likely that the Jovian ring is also shaped by interactions with small satellites such as the newly discovered J XIV.

Each planetary ring system is found close to its parent planet. Presumably, the ring material lies close to or within the Roche limit, and that is why it does not rapidly collect into satellites. The condition that the rings are located near the Roche limit tells us that $\rho \approx M_p/r^3$ or $G\rho \approx \Omega^2$.

The random velocities and particle sizes in planetary disks are not well determined. Dynamical considerations (Brahic 1977; Goldreich and Tremaine 1978*a*) imply that $c \gtrsim \Omega b$ and suggest that $c \approx \Omega b$ may often apply. However, the latter relation should be used with caution since the random velocities may be enhanced by satellite interactions near resonances (cf. § V*c*), by gravitational scattering due to atypically large ring particles (Cuzzi *et al.* 1979), and, for small particles, by electrostatic repulsion which inhibits physical collisions at low velocities.

The relations $G\rho \approx \Omega^2$ and $c \approx \Omega s$ may be used to simplify the equations derived earlier in this section. Here we merely point out that they imply $Q \approx \tau^{-1}$.

e) *Eccentricity Evolution*

In § II*e* we showed that torques due to $l = m \pm 1$ corotation resonances damp the satellite's orbital eccentricity while those due to $l = m \pm 1$ Lindblad resonances excite it. When all of the resonances are unsaturated, the net result is that the eccentricity damps. However, the corotation resonances are easier to saturate than the Lindblad resonances. This saturation arises because of trapping of the particles' orbital angular velocity into libration about the pattern velocity. When the strongest corotation resonances are saturated and the Lindblad resonances are not, the orbital eccentricity will grow to some finite value. This process will be discussed further in a subsequent paper.

VI. APPLICATIONS

In this section we present an illustrative application of our results to the interaction of Jupiter with the protoplanetary nebula. We assume that Jupiter's mass and orbital radius have their present values: $M_{2\downarrow} = 0.001\, M_\odot = 2 \times 10^{30}$ g, $a_{2\downarrow} = 5.2$ AU $= 7.8 \times 10^{13}$ cm. Jupiter's mean motion is $\Omega = 1.7 \times 10^{-8}\ \mathrm{s}^{-1}$. The appropriate value for the nebular surface density is less certain. If the condensed matter now in the terrestrial planets represents a mass fraction $\sim 5 \times 10^{-3}$ of the original nebula, then the mean surface density inside Jupiter's orbit was $\sim 130\ \mathrm{g\ cm}^{-2}$. If we spread Jupiter's mass uniformly over an annulus between $\frac{1}{2}a$ and $\frac{3}{2}a$, we obtain $\Sigma = 50\ \mathrm{g\ cm}^{-2}$. These are conservative estimates of the nebular surface density in the neighborhood of Jupiter. Thus, we will express our results in units of $\Sigma_{100} = \Sigma/100\ \mathrm{g\ cm}^{-2}$, recognizing that $\Sigma_{100} \gtrsim 1$. Similarly, we write the nebular temperature in units of $T_{100} = T/100$ K. The sound speed for molecular hydrogen is $c = 7.6 \times 10^4 T_{100}^{1/2}\ \mathrm{cm\ s}^{-1}$.

Toomre's stability parameter (eq. [84]) for the disk is $Q \approx 60 T_{100}^{1/2} \Sigma_{100}^{-1}$. Thus the self-gravity of the disk is unimportant. In this case the maximum azimuthal wavenumber which contributes to the torque on Jupiter (cf. eq. [93]) is $m_{\max} = 0.69\Omega a/c \approx 12 T_{100}^{-1/2}$. The distance of the corresponding Lindblad resonance from Jupiter is $|a - r|/a \approx 2/(3m_{\max}) = 0.06 T_{100}^{1/2}$.

The scale of the density waves excited at the resonances is relatively large. From equation (100) the radial interval Δr_1 occupied by the first cycle is given by $\Delta r_1/a = 0.46 m^{-1/3} T_{100}^{1/3}$. For $m = m_{\max}$, $\Delta r_1/a = 0.2 T_{100}^{1/2}$. Clearly, the temperature of the nebula is sufficiently high that our approximation $c \ll \Omega a$ (cf. § II*a*) is not very good; nevertheless our formulae are still useful for rough estimates of the torques on Jupiter.

The molecular viscosity of the nebula is negligible. Therefore, the viscous damping length l_V (eq. [97]) depends on whether the nebula is turbulent. If it is turbulent, and we write $\nu = \alpha c^2/\Omega$, $\alpha < 1$ for the turbulent viscosity, we find

$$l_V/a \approx 0.15 \alpha^{-2/3} m^{-1/3} T_{100}^{1/3}\,. \tag{107}$$

By contrast, the distance between resonances for $m \gg 1$ is $\Delta r/a \approx 2/3m^2$. In the region where the torques are strongest, $m \approx 12$, $\Delta r \lesssim l_V$. Thus the spatial variation of the angular momentum transferred to the disk is smooth, even if there is strong ($\alpha \sim 1$) turbulent viscosity.

Finally, we must check that our linear approximation is correct. A rough criterion for the validity of the linear approximation is that the radial velocity u should be subsonic at the resonance. From the solutions in GT1 we find the maximum value of u/c at the Lindblad resonance to be

$$\max\left[\frac{u}{c}(r_L)\right] = 1.0 \frac{M_s}{M_p} m^{1/3} \left(\frac{\Omega r}{c}\right)^{5/3} = 0.12 m^{1/3} T_{100}^{-5/6} = 0.27 T_{100}^{-1} \qquad \text{for } m = m_{\max}. \tag{108}$$

Thus, the perturbations are linear at the resonance.

With these preliminaries we may apply equation (30) to estimate the time scale over which Jupiter's semimajor axis evolves. We replace the ring mass M_r by $2\pi r \Sigma dr$ and integrate over r up to $|a - r| = 2a/3m_{\max}$. For $m_{\max} \gg 1$, we find

$$\frac{1}{a}\frac{da}{dt} = \pm 5.6 \left(\frac{M_s}{M_p}\right)\left(\frac{\Sigma a^2}{M_p}\right) \Omega m_{\max}^3\,. \tag{109}$$

The $\pm$ sign refers to the contribution from the parts of the disk interior and exterior to the satellite, respectively. With our scant knowledge of the nebula we cannot be certain whether the interior or exterior torque is larger. Thus, we can estimate only the magnitude of the effect, not its sign. For the parameters we have adopted here $a^{-1}da/dt = \pm \tau_a^{-1}$, where the characteristic time $\tau_a = 6 \times 10^2\ \mathrm{yr}\ \Sigma_{100}^{-1} T_{100}^{3/2}$. Since most of the torque comes from the parts of the disk with $|a - r|/a \sim m_{\max}^{-1}$, we expect that gradients in the disk properties will always lead to a residual torque which is at least $m_{\max}^{-1}$ times the torque from one side of the disk. Thus, Jupiter's semimajor axis will evolve on a time scale $\lesssim m_{\max} \tau_a \sim 7 \times 10^3\ \mathrm{yr}\ \Sigma_{100}^{-1} T_{100}$.

Similarly, we can estimate the time scale for the damping of Jupiter's eccentricity by the disk from equation (31):

$$\frac{1}{e}\frac{de}{dt} = -2 \times 0.59 \left(\frac{M_s}{M_p}\right)\left(\frac{\Sigma a^2}{M_p}\right) \Omega m_{\max}^4\,. \tag{110}$$

The factor 2 is a reminder that both the interior and exterior contribute to the eccentricity damping. If we write $e^{-1}de/dt = -\tau_e^{-1}$, we find $\tau_e = 3 \times 10^2$ yr $\Sigma_{100}^{-1} T_{100}^2$. Note that τ_e is somewhat less certain than τ_a since the cutoff $m_{\max}$ was calculated only for the $l = m$ Lindblad resonances which are the most important for τ_a, not for the $l = m \pm 1$ Lindblad resonances and $l = m$ corotation resonances which make the dominant contribution to τ_e.

VII. SUMMARY

We have calculated the rate at which angular momentum and energy are transferred between a disk and a satellite. The main approximations are: (1) we use linear perturbation theory; (2) we assume that the eccentricity of the satellite is small, and (3) we assume that the disk is thin, i.e., $c \ll \Omega R$.

The calculations are done by independent methods in §§ II and III. The main results are: the rate of change of the satellite's semimajor axis (eqs. [28] and [65]) and the rate of change of the satellite's eccentricity (eqs. [29] and [74]). These equations yield the contribution from a single ringlet of mass M_r and negligible radial extent; the total contribution from a disk is obtained by summing the effects of many ringlets.

In general, torques from Lindblad resonances increase the satellite's eccentricity while those from corotation resonances damp it; to lowest order in e the corotation torques are slightly larger in a Kepler disk (eq. [31]), and the eccentricity damps in the absence of saturation.

If the satellite is embedded in a disk, torques from resonances with azimuthal wavenumber $m \gg m_{\max} = \mu_{\max}\Omega R/c$ are not important (§ IV). For Kepler disks, $\mu_{\max} = 0.69$ for $Q = \infty$ and $\mu_{\max} = 1.45$ for $Q = 2$. The torque on the disk cuts off for $|a - r| \lesssim a\kappa/(2|A|m_{\max})$ (eqs. [28], [30], and [65]).

This research was supported in part by NSF grants PHY-79-19884 and AST-79-24978, and NASA grant NGL-05-002-003.

REFERENCES

Brahic, A. 1977, *Astr. Ap.*, **54**, 895.
Chandrasekhar, S. 1960, *Principles of Stellar Dynamics* (New York: Dover), p. 156.
Cuzzi, J. N., Durisen, R. H., Burns, J. A., and Hamill, P. 1979, *Icarus*, **38**, 54.
Franklin, F. A., Lecar, M., Lin, D. N. C., and Papaloizou, J. 1979, preprint.
Goldreich, P., and Lynden-Bell, D. 1965, *M.N.R.A.S.*, **130**, 125.
Goldreich, P., and Tremaine, S. 1978*a*, *Icarus*, **34**, 227.
———. 1978*b*, *Icarus*, **34**, 240 (GT1).
Goldreich, P. and Tremaine, S. 1978*c*, *Ap. J.*, **222**, 850 (GT2).
———. 1979*a*, *Nature*, **277**, 97.
———. 1979*b*, *Ap. J.*, **233**, 857 (GT3).
Julian, W. H., and Toomre, A. 1966, *Ap. J.*, **146**, 810.
Lin, D. N. C., and Papaloizou, J. 1979, *M.N.R.A.S.*, **186**, 799.
Lynden-Bell, D., and Kalnajs, A. J. 1972, *M.N.R.A.S.*, **157**, 1.
Mark, J. W. K. 1976, *Ap. J.*, **205**, 363.
Spitzer, L., and Schwarzschild, M. 1953, *Ap. J.*, **118**, 106.
Toomre, A. 1964, *Ap. J.*, **139**, 1217.

PETER GOLDREICH: Mail Code 170-25, California Institute of Technology, Pasadena, CA 91125

SCOTT TREMAINE: School of Natural Sciences, Institute for Advanced Study, Princeton, NJ 08540